Title: Mesoporous silica and carbon based catalysts for esterification and biodiesel fabrication — the effect of matrix surface composition and porosity

Author: <ce:author id="aut0005" author-id="S0926860X17300078-b64ed8dc253baa602b56fdce2532bb81"> Emma M. Björk<ce:author id="aut0010" author-id="S0926860X17300078-2fc06d964798adcaf11510b9231f494d"> María P. Militello<ce:author id="aut0015" author-id="S0926860X17300078-006d70f5e69c778452fd6f6fd9c7fffe"> Luciano H. Tamborini<ce:author id="aut0020" author-id="S0926860X17300078-49fd98d9277d925c98525bfa9bc72140"> Rusbel Coneo Rodriguez<ce:author id="aut0025" author-id="S0926860X17300078-a3a850b2f2b692ad2e2ca3f17b10c7c2"> Gabriel A. Planes<ce:author id="aut0030" author-id="S0926860X17300078-d0e0976cea249f8fdd080b31904b3742"> Diego F. Acevedo<ce:author id="aut0035" author-id="S0926860X17300078-0b8ed36d1521538c399edaa0450e5c7b"> M.Sergio Moreno<ce:author id="aut0040" author-id="S0926860X17300078-3f339287609492d7faaa171f417e300a"> Magnus Odén<ce:author id="aut0045" author-id="S0926860X17300078-7607f4feba74c71bea2322dead18b23a"> Cesar A. Barbero

PII: S0926-860X(17)30007-8
DOI: http://dx.doi.org/doi:10.1016/j.apcata.2017.01.007
Reference: APCATA 16118

To appear in: *Applied Catalysis A: General*

Received date: 16-9-2016
Revised date: 17-12-2016

Accepted date: 9-1-2017

Please cite this article as: Emma M.Björk, María P.Militello, Luciano H.Tamborini, Rusbel Coneo Rodriguez, Gabriel A.Planes, Diego F.Acevedo, M.Sergio Moreno, Magnus Odén, Cesar A.Barbero, Mesoporous silica and carbon based catalysts for esterification and biodiesel fabrication — the effect of matrix surface composition and porosity, Applied Catalysis A, General http://dx.doi.org/10.1016/j.apcata.2017.01.007

Mesoporous silica and carbon based catalysts for esterification and biodiesel fabrication – the effect of matrix surface composition and porosity

Emma M. Björk[1,2 *], María P. Militello[2], Luciano H. Tamborini[2], Rusbel Coneo Rodriguez[2], Gabriel A. Planes[2], Diego F. Acevedo[2,3], M. Sergio Moreno[4], Magnus Odén[1], and Cesar A. Barbero [2]

[1] *Nanostructured Materials, Department of Physics, Chemistry and Biology (IFM), Linköping University SE-58183 Linköping, Sweden*

[2] *Departamento de Química, CONICET, Facultad de Ciencias Exactas, Fisicoquímicas y Naturales, Universidad Nacional de Río Cuarto, Ruta 36 Km 601, 5800, Río Cuarto, Argentina*

[3]*Departamento de Tecnología Química. Facultad de Ingeniería, Universidad Nacional de Río Cuarto, Ruta 36 Km 601, 5800, Río Cuarto, Argentina.*

[4] *Departamento de Materiales Metálicos y Nanoestructurados. Centro Atómico Bariloche-CONICET. Av. Bustillo 9500, 8400 - San Carlos de Bariloche, Argentina*

***Corresponding author**: E-mail: emma.bjork@liu.se; Phone: +46 (0)13 28 25 43

Graphical abstract

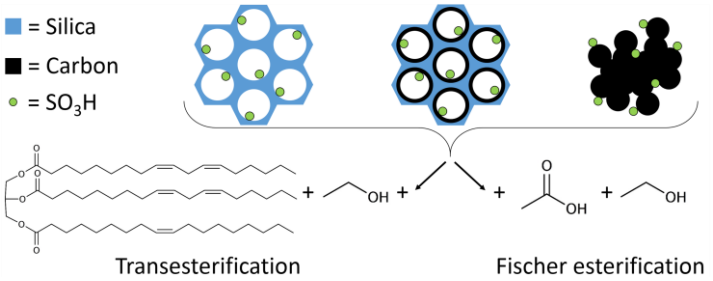

Highlights

- The effect of catalyst matrix composition and porosity was studied in Fischer esterification and transesterification using several mesoporous silica/carbon supports.
- In Fischer esterification with acetic acid and ethanol, both silica and carbon matrixes are effective, but an ordered porosity outperforms disordered porosity due to diffusion effects.
- In biodiesel production, a matrix mixture of carbon nanoparticles and mesoporous silica gives a mass yield of 85 % while pure silica and carbon matrixes gives a yield of 0 % and ~30 % respectively.
- A suitable choice of catalyst matrix in terms of porosity and composition strongly affects the product yield and reaction rate, and this knowledge can be transferred to other systems.

Abstract

The effects of catalyst matrix porosity composition on the catalytic performance have been studied using sulfonated mesoporous SBA-15 silica. The matrix was sulfonated with three different methods: grafting, *in situ* oxidation, and carbon infiltration. Additionally, unordered sulfonated mesoporous carbon, and the commercial catalysts Amberlite IR-120 and Nafion 117 were tested. The catalytic performance was evaluated in a Fischer esterification using acetic acid and ethanol, as well as in a transesterification of triglycerides (sunflower oil) and ethanol to produce biodiesel. The study shows that for long carbon chains, the effective wetting of the porous catalyst matrix by the reactants is most important for the catalytic efficiency, while for shorter carbon chain, the mass transport of the reagents trough the porous structure is more important. The catalysts were analysed using electron microscopy and physisorption. The study shows that the reactions are faster with carbon infiltrated materials than the silica materials due to a higher concentration of sulfonic groups linked to the carbon. The *in situ* functionalized SBA-15 is a more efficient catalyst compared to the post grafted one. All the synthesized catalysts outperform the commercial ones in both reactions in terms of conversion.

Keywords: Mesoporous silica, Mesoporous carbon, Fischer Esterification, Biodiesel, Transesterification

1. Introduction

Esterification is an industrially important process used for pharmaceutics, food, flavour, and biofuels (biodiesel). Finding a cheap and efficient route to produce biofuel is currently an important task to address the environmental concern footprint and cost of fossil fuels. Biodiesel is constituted by alkyl esters of fatty acids. It is usually produced by transesterification of natural fats (vegetal oils or animal fats) with methanol or ethanol. The reaction is slow and requires basic or acid catalysis. Today, different types of catalysts are used, such as alkalis or mineral acids. However, some drawbacks limit their use. For example, base catalysts (e.g. KOH), produces soap as a side product [1]. Such alkalis also tend to adsorb water during storage which further diminishes their catalytic performance [2]. Acids such as H_2SO_4 and HCl are used as homogenous catalysts, but are difficult to separate from the products and cause equipment corrosion and toxic waste [3]. To overcome these problems, acid heterogeneous catalysts with sulfonic acid groups on different matrixes, such as mesoporous and hierarchic materials [4], zeolites [5], disordered nanoporous carbons [6], and supermicroporous polymers [7, 8], have been developed.

Mesoporous silica with cylindrical pores, such as SBA-15 [9], has been used as porous matrix for several catalysts, and especially silica functionalized with propyl sulfonic acid has been shown to be an efficient catalyst in organic reactions [3, 10]. The material can be synthesized with a wide range of characteristics that affect their performance in the esterification process, e.g. pore size [11] , pore structure [12], and particle morphology [13]. SBA-15 particles can also be grown onto surfaces [14] as solid heterogeneous catalysts, which can easily be removed from the reaction solution and reused. The transesterification rate will decrease with longer alkyl chains, which is a result of the interaction between the reactants and the catalyst surface [15]. To enhance the performance of silica based catalysts, organic groups can be grafted onto the silica surface together with the sulfonic groups. An alternative to grafting is to form a CMK-5 material by depositing a thin carbon layer on the pore walls of the mesoporous silica [16]. CMK-5 is naturally hydrophobic, but when it is functionalized with sulfonic acid groups it becomes more hydrophilic. Such catalyst can be considered as a hydrophobic substrate with hydrophilic functional groups, which are stable during esterification [17].

Since many characteristics of the catalyst matrix affect the catalytic performance it is crucial to optimize them for the reaction. The balance of the interaction between the reagents and the catalyst surface must be weighed against the diffusion possibilities to find the best catalyst matrix. Resin-based carbons are alternatives to the more expensive ordered mesoporous carbon. It has been shown that porous carbons synthesized in a sol-gel reaction with resorcinol and formaldehyde perform well as catalysts for biodiesel production [18]. However, since there is a lack of interconnecting pores in this

material, it is suitable for comparison with the CMK-5 to determine the key mechanism for finding the preeminent matrix.

In the present study, several high yield catalysts based on sulfonated mesoporous structures are presented. Most of them are based on mesoporous silica of SBA-15 type, with a monodispersed rod morphology [19, 20] to favour diffusion. The rods were either sulfonated during or after the SBA-15 synthesis. Carbon infiltration was performed using two different methods, and then sulfonated. In addition, unordered porous carbon and commercial catalysts are used as benchmarks. With this range of prepared catalysts, the effects of porosity and matrix hydrophilicity on the catalytic conversion are reported. The catalysts are tested in Fischer esterification of acetic acid and ethanol, as well as biodiesel production (transesterification) from sunflower oil triglycerides and ethanol. The results emphasise the importance of a proper matrix choice for the catalytic group, and how the hydrophilicity and pore structure affects the catalytic performance.

2. Experimental methods

2.1 *Synthesis*

For the syntheses, HCl (Cicarelli), Poly(ethylene glycol)-block-poly(propylene glycol)-block-poly(ethylene glycol) M_n ~ 5800 g/mol (P123) (Aldrich), ammonium fluoride (Sigma-Aldrich), heptane (Sigma-Aldrich), tetraethyl orthosilicate (TEOS), resorcinol (Sigma-Aldrich), (3-Mercaptopropyl)trimethoxysilane (MPTMS) (Aldrich), formaldehyde (Cicarelli), cationic polyelectrolyte (poly(diallyl, dimethylammonium chloride) (PD) (BDH), and sodium carbonate (Cicarelli) were used as received.

2.1.1 SBA-15 synthesis

Monodispersed SBA-15 particles were synthesized using the route described by Björk *et al*. [20]. In a typical synthesis, 4.8 g of P123 and 40 mg NH_4F were dissolved in 160 nm of 1.84 M HCl. When the reagents had dissolved, 2 mL of heptane was premixed with 11 mL of TEOS, and this mixture was added to the micellar solution under vigorous stirring for 4 min at 20 °C. After this, the stirring was turned off and the synthesis was kept under static conditions for 20 h. The solution was then transferred to a TPFE flask and hydrothermally treated at 100 °C for 24 h. The final product was collected by filtration, washed with distilled water, dried in room temperature overnight, and finally calcined at 550 °C for 5 h with a ramp of 1 °C/min. This material is labelled SBA-15.

2.1.2 Post-sulfonation (SBA-15-PS)

SBA-15 with sulfonic groups was synthesized by controlled functionalization of the mesoporous surface. This was achieved by linking thiol groups trough the reaction of the as prepared SBA-15 with

a functionalized silane (mercaptopropylsilane, MPTS) followed by oxidation of the thiol group using H_2O_2 to sulfonic acid.

The matrix material was synthesized using a SBA-15 protocol where the P123 template was removed by H_2O_2 oxidation [21], instead of calcination in order to enhance the number of silanol groups. The SBA-15 was then sulfonated using the protocol from Pirez *et al.* [22]. In a typical synthesis, 0.5 g of SBA-15 was mixed with 0.5 mL of MPTMS and 15 mL of Toluene. This mixture was stirred under reflux at 130 °C for 24 h. The material was collected using centrifugation and was washed with ethanol prior to drying in a furnace at 80 °C. The thiol groups were then converted into sulfonic acid groups by oxidation with 15 mL H_2O_2 for 24 h in room temperature. The product was then centrifuged, washed with ethanol, and dried over night at 80 °C.

2.1.3 Direct sulfonation (SBA-15-DS)

SBA-15 materials bearing sulfonic groups were also synthesized by *in situ* oxidation of thiol groups in the matrix by addition of MPTS and H_2O_2 during the SBS-15 material formation.

The direct sulfonated SBA-15 was synthesized using a modified route from Margolese *et al.* [23]. Half batch size of the SBA-15 synthesis described above was used. 20 min into the static time of the SBA-15 synthesis, 0.5 mL of MPTMS and 0.8 mL of H_2O_2 30 % were added to the synthesis solution. The mixture was gently stirred just to mix in the new reactants, and then static conditions were kept for 20 h. The solution was then hydrothermally treated at 100 °C for 24 h. The material, labelled SBA-15-DS, was collected by filtration, and the template removed by oxidation with H_2O_2 [21]. The material was washed with deionized water and dried over night at 80 °C.

2.1.4 Carbon infiltration using furfuryl alcohol (SBA-15-Carb1/2)

1 g of SBA-15 was mixed with 1 mL (SBA-15-Carb1) or 2 mL (SBA-15-Carb2) of furfuryl alcohol. The mixture was then put in vacuum to assure an even distribution of the furfuryl alcohol into the mesopores. The alcohol was polymerized at 90 °C for 1 h. Finally, the polymer was pyrolyzed in argon atmosphere at 800 °C for 1 h with a heating rate of 40 °C/min, to form a thin carbon layer on the pore walls.

2.1.5 Carbon infiltration using resorcinol (SBA-15-RFC)

1 g of SBA-15 was mixed with 0.6 g of resorcinol dissolved in 60 mL of deionized water. The mixture was stirred at ambient temperature for 2 h to adsorb the resorcinol in the pores. The particles were separated by centrifugation and washed with deionized water. The composite was dried at 80 °C overnight. The material was then exposed to vapours of formaldehyde and ammonia (catalyst) for 24

h to form the resorcinol/formaldehyde resin. The material was then pyrolyzed in argon atmosphere at 800 °C for 1 h under argon atmosphere with a heating rate of 40 °C/h to form carbon particles.

2.1.6 Unordered porous carbon (PC)

The unordered porous carbon was synthesized following the protocol by Bruno *et al.*[24]. Monolithic porous carbons were synthesized by polycondensation of resorcinol (R) with formaldehyde (F) in the presence of PD as pore stabilizer and sodium carbonate (C) as basic catalyst. The molar ratio of resorcinol to formaldehyde (37 % wt in an aqueous solution) (R/F) and the ratio of resorcinol to water (R/W) were both fixed at 0.5 g/mL. Furthermore, the PD/R ratio was kept constant at 7 and (R/C) at 200. All components were mixed and stirred for 10 minutes. Then the samples were polymerized by heating at 70 °C, in a closed system, for 24 h. to obtain a porous organic gel. The organic gel was dried in air for 6 h at 70 °C. Finally, porous carbons (PCs) were obtained by pyrolysis of the dried monolithic gels at 800 °C for 1 h under argon atmosphere with a heating rate of 40 °C/h.

2.1.7 Sulfonation of carbon containing materials

All carbon containing materials (ordered and unordered) were sulfonated using concentrated (98%) sulphuric acid. 0.2 g of matrix material was added to 10 mL of H_2SO_4 . The mixture was heat treated for 8 h at 80 °C under reflux and then cooled to room temperature. The samples were carefully washed with distilled water and separated by centrifugation. The washing was repeated until the washing solution reached neutral pH. In that way, the black precipitate was isolated [25, 26]. Finally, the sulfonated carbon containing materials were dried at 80 °C overnight.

2.2 ***Characterization***

2.2.1 Materials Characterization

Nitrogen sorption isotherms were obtained using a Micromeritrics ASAP 2020 at -196 °C with samples degassed at 200 °C. The specific surface area was determined with the BET method at $P/P_0 = 0.1 – 0.2$. The pore size was calculated using the KJS method [27] at the adsorption isotherm for the silica based materials, and the BJH method [28] for the unordered porous carbon. The total pore volume was estimated at $P/P_0 = 0.98$. Small angle x-ray diffraction (SAXRD) was performed on a PANAlytical Empyrean in transmission mode using Cu K_α radiation. Scanning electron microscopy (SEM) was performed with a Leo 1550 Gemini Scanning Electron Microscope operated at 3 kV and a working distance of 3 – 5 mm. Transmission electron microscopy (TEM) was performed with a FEI Tecnai G2 F20 UT microscope operated at 200 kV to observe the porous structure of the materials, and energy dispersive x-ray spectroscopy (EDS) to identify the position of the sulfonic acid groups. TEM specimens were prepared by dropping the materials on a lacey carbon grid without using sonication. Prior to the EDS analysis of the sulfonated materials, they were treated with a 0.1 M $BaCl_2$ solution. The relative

wettability by the hydrophobic reactant (sunflower oil) [29, 30] was evaluated by turbidimetry [31]. 1 mg of each catalyst powder was sonicated with 2 ml sunflower oil for 15 min, and immediately afterwards, the light extinction was measured in a spectrophotometer (Hewlett-Packard 8453 diode array UV-visible spectrophotometer) at 700 nm, as a function of time. To avoid the interference of differences in light absorption, the extinctions are normalized to the maximum extinction and the precipitation kinetics is used as indication of wettability [32].

2.2.2 Determination of number of catalytic groups

Determination of sulfonic acid groups was performed using acid-base titration. For the silica samples, 0.10 g of the material was mixed with 10 mL deionized water and the amount of acidic groups was determined using direct titration with 0.10 M NaOH solution. For all carbon containing samples, 0.10 g of the materials were mixed with 10 mL 0.1 M Na_2SO_4 to react with the sulfonic groups, forming bisulfate [33]. This solution was stirred for 4 h prior to titration with a 0.10 M NaOH solution. The bisulfate groups in solution react with the NaOH giving the total amount of sulfonic acid groups. Other acid groups (carboxylic, phenolic, lactonic) are less acid than sulphate and do not give bisulfate upon exposure to sulphate ions [18]. The standardization of the NaOH solution was performed using potassium phthalate monoacid as primary standard and a digital pH meter. Eq 1 was used to calculate the amount of acidic groups.

$$n_{ac} = V_{NaOH} \cdot [NaOH] \qquad \text{Eq. 1}$$

Where n_{ac} is the moles of acid groups, V_{NaOH} is the volume used in the titration and [NaOH] is the base concentration used in the titration.

2.2.3 Fischer esterification of acetic acid with ethanol

The performance of the synthesized catalysts was tested in esterification of acetic acid with ethanol. In the reaction 50 mL ethanol and 20 mL of acetic acid was mixed with 0.1 g of the catalyst. The reaction was carried out at 80 °C under constant stirring and reflux for 8 h. The reaction mixture was continuously sampled by removing 1 mL aliquots and mixing it with 1 mL of distilled water to terminate the reaction. The acetic acid conversion was determined by direct titration using 0.2 M NaOH. The equivalence point was found using a pH electrode. The conversion was calculated using Eq 2.

$$X(\%) = \frac{molHAc_{initial} - molHAc_{end}}{molHAc_{initial}} \cdot 100 \qquad \text{Eq. 2}$$

Where $molHAc_{initial}$ is the initial moles of acetic acid, $molHAc_{end}$ is the moles of acetic acid at different times.

2.2.4 Transesterification of sunflower oil triglycerides with ethanol

Some catalysts were also tested in the transesterification of sunflower oil triglycerides and ethanol to produce biofuel. In the reaction, 2.75 mL of sunflower oil was mixed with 3.3 mL of ethanol and 0.25 g of catalyst. The reaction was performed at 90 ° under constant stirring and reflux for 8 h. After the reaction, the mixture was centrifuged to remove the catalyst from the reaction medium. Subsequently, the supernatant liquid consisted of two immiscible phases, one oil phase and one alkyl-rich phase. The volume and density of the alkyl-rich phase was determined, and further analysed by gas chromatography (GC) to determine the total amount of fatty acid ethyl esters (FAEE) in the product and its composition. These data were used to calculate the mass of the phase recovered and finally the reaction yield. The FAEE yield percentage was calculated using [34]

$$\%FAEE\ yield = \frac{weight\ of\ biodiesel}{weight\ initial\ oil} \cdot 100 \qquad \text{Eq. 3}$$

For gas chromatography, a Hewlett Packard 5890 Series II coupled to a mass detector 5972 series of the same brand was used. The ionization energy was 70 eV. The oven temperature was programmed as follows: initial temperature 60 ° C, final temperature 260 ° C, with a heating rate of 4 ° C / min. Helium carrier gas was used at the rate of 0.8 mL / min. The injector temperature was 200 ° C and column head pressure was 5 psi. For the analysis, 60 µL of product, 10 µL of dodecane, and 6 mL of hexane were premixed, and 0.1 µL of this mixture was injected to the chromatograph.

3. Results and discussion

3.1 The materials

It has been shown that the presence of additives (fluoride ions, heptane) can be used to change the shape of SBA-15 nanoparticles and its porosity [19-21]. Since in some cases the synthetic procedure necessary to incorporate catalytic acid groups require the addition of other precursors (e.g. MPTS) it is necessary to evaluate their effect on the particle morphology. In those cases when carbon is incorporated after the silica synthesis to anchor the catalytic acid groups, it is relevant to determine if the carbon coats the internal mesoporous walls or just the outside of the particles.

Scanning electron micrographs of the synthesized materials are shown in Figure 1. The original SBA-15 consists of discrete ~400 x 400 nm^2 large particles. The materials infiltrated with carbons have the same morphology, with no external carbon particles visible. SBA-15-DS (Figure 1 (b)), which was

functionalized during the particle synthesis, consists of more narrow particles, with the same length as the SBA-15. This indicates that MPTMS and H_2O_2 either affect the extension of the PEO chains into the aqueous solution [20], or that the functional groups passivate the –OH groups on the silica surface, and limit side by side attachment of the elongated micelles [35]. The latter is most probable, since the MPTMS will exchange the silanol groups with thiol groups, and prohibit further condensation bonding between the micelles. The unordered carbon (Figure 1 (f)) consists of large monoliths composed of clusters of nanoparticles.

Transmission electron micrographs in Figure 2 show that all SBA-15 based materials have cylindrical pores with hexagonal order. This indicates that the infiltration of furfuryl alcohol to form a CMK-5 like structure [16] is successful, and that the pore walls are coated with a thin layer of carbon in SBA-15-Carb2. No excess carbon can be observed in the TEM micrographs (Figure 2 (b)). In SBA-15-RFC (Figure 2 (c)), there are two phases present, the hexagonal silica structure, as well as small darker particles. Since it is difficult to directly detect carbon by EDS, due to its low atomic number, the sulfonated materials were immersed in $BaCl_2$ which reacts with the sulfonic groups. Therefore, a map of Ba should be equivalent to a map of sulfonic groups.

Representative EDS spectra, Figure 2, shows Ba present in all SBA-15-DS and SBA-15-Carb2 particles, meaning that the sulfonic functionalization is homogenous throughout the material. For SBA-15-RFC, Ba is only present in the darker particles, which we infer to be RFC particles. There is no indication of sulfonated carbon within the SBA-15-RFC mesopores. It means that the SBA-15-RFC synthesis resulted in a mixture of unsulfonated SBA-15 mixed with sulfonated RFC nanoparticles. PC, which is the only non SBA-15 based material, is shown in Figure 2 (d). This material consists of aggregated carbon particles, and the porosity stems from cavities between the particles.

The physisorption isotherms in Figure 3 (a) show that all SBA-15 based materials have type IV isotherms with type 1 hysteresis loops, indicative of ordered, cylindrical pores, typical for SBA-15. The materials have also narrow pore size distributions, shown in Figure 3 (c) and (d). The PC material has a type 3 hysteresis loop, typical for aggregates and in agreement with the TEM results. All data derived from the isotherms (pore size, specific surface area, and total pore volume) are presented in Table 1.

The pore size is larger for SBA-15-PS and SBA-15-DS compared to the original SBA-15, see Figure 3(b). The removal of P123 for original SBA-15 was done by calcination and by oxidation in H_2O_2 for SBA-15-PS and SBA-15-DS. Calcination is known to cause shrinkage of the silica, which is not the case for oxidation in H_2O_2. Oxidation in H_2O_2 also increase the number of silanol groups in SBA-15-PS [36], and keeps the thiol and sulfonic acid groups on the pore surfaces [37]. The physisorption data also shows that the furfuryl alcohol infiltration forms thin carbon cylinders on the mesopore walls in SBA-15-Carb1

and SBA-15-Carb2. There are no indications of plugs or intrusions in the pores in the hysteresis lopes. The pore size is reduced to 9.2 and 8.9 nm with increasing furfuryl alcohol amount. Considering this, we conclude that our method is a simple way to form CMK-5 carbons in large pore SBA-15. However, in this study the silica template for the CMK-5s is not removed. It is kept to avoid adding extra diffusion paths in the catalyst through the additional pores in a pure carbon replica.

In SBA-15-RFC, the mesopore size is similar to the parent SBA-15 material, while the specific surface area and total pore volume are significantly reduced (see Table 1). This is due to the presence of carbon particles mixed with the SBA-15. The carbon particles are likely to be dense and do not contribute to the surface area. The carbon particles increase the total mass, which results in a reduced specific surface area and total pore volume. However, the weight gain of 7.6 % is not sufficient to completely explain the large reduction of these parameters. Some of the carbon is expected to also be present inside the mesopores since the mesopore size is reduced, even though there are no noticeable amounts of sulfonic groups in the pore channels.

X-ray diffractograms for all catalysts are presented in Figure 3 (b). All SBA-15 based catalysts show three peaks which correspond to the hexagonal pore order in the material. The PC sample shows no diffraction peaks, indicating a disordered pore structure. The unit cell parameters calculated from the diffraction peaks are presented in Table 1. It is clear that the silica based materials has a large unit cell parameter compared to the carbon infiltrated ones. This is due to shrinkage of the unit cell parameter upon heat treatment, e.g. calcination, compared to the H_2O_2 treated materials [36].

Figure 4 shows the TGA curves of the carbon infiltrated samples, SBA-15-Carb1, SBA-15-Carb2, and SBA-15-RFC. All samples show a slight mass reduction when the material is heated to 100 °C, which is attributed to the loss of water. The carbon starts to oxidize above 500 °C. At 620 °C, the carbon is completely lost and only the parent SBA-15 material remains. The amount of carbon was determined as

$$m_{carbon} = \frac{m_{mix} - m_{SBA}}{m_{SBA}} \quad \text{Eq.4}$$

where m_{mix} is the mass of the material after water removal as determined from the first plateaus in Figure 4. The results are given in Table 1. It is apparent that doubling the amount of furfuryl alcohol almost doubles the amount of carbon in the final product, i.e. comparing SBA-15-Carb1 and SBA-15-Carb2.

The number of acidic sites was determined by direct titration with NaOH. For both of the sulfonated SBA-15s, the number of acidic sites is very similar, independent whether the functionalization was performed during or after the material synthesis. It should be noted that in the SBA-15-PS, the sulfonic

groups are all present on the material surface, while for the SBA-15-DS acidic groups can be present also in the silica wall. The amount of MPTMS added during the reaction correspond to an amount of ~ 1.92 mmol/g acidic sites in the silica, and it is hence most likely that additional sulfonic acid groups are present in the bulk of SBA-15-DS that are not detected from the titration. More sulfonic groups are present in the carbon based materials compared to the silica ones. Sulfonation is expected to occur on the silanol groups in the silica materials while it occurs across the entire carbon surfaces. Hence, the number of silanol-groups limits the sulfonation of silica, which is why we see less acidic sites in the silica based materials.

SBA-15-Carb2 has a significantly lower amount of acidic sites compared to SBA-15-Carb1, 0.59 and 0.87 mmol/g respectively. This is due to thicker, less porous carbon walls resulting in less available surface area. It should be noted that the treatment with sulfuric acid only affects the carbon surfaces, not the silica. Materials containing both SBA-15 and carbon also have silanol groups on the silica surface, and as will be shown, affect the catalytic performance even though they are not an active in the catalytic reaction.

The disordered carbon, PC, has a lower concentration of sulfonic groups compared to the other carbon based materials, although the specific surface area is large. A large part of this surface is generated by the disordered micropores, in which the diffusion is poor. The sulfonic acid penetrates these micropores less effectively compared to the larger mesopores, and as a result the micropore walls are sulfonated to a lower degree.

3.2 Catalytic activity during Fischer esterification

The catalysts were tested for Fischer esterification of acetic acid with ethanol using a molar ratio of acid to alcohol 1:2.5 at 80 °C. The acetic acid conversion is presented in Figure 5. For comparison, the reaction was also performed in the presence of non-functionalized SBA-15 and of two commercial solid acid catalysts (Nafion®117 and Amberlite IR-120). Figure 5 shows that the entire lot of synthesized materials exhibit enhanced catalytic effects compared to the parent SBA-15 material.

The *in situ* functionalised silica material, SBA-15-DS, is a more effective catalyst compared to the post functionalised SBA-15-PS, even though the number of acidic sites are the same (Table 1). The pore widths and lengths are similar for these materials, which should yield a comparable diffusion within the pores. Instead, the most probable reason for the discrepancy is the attachment of the sulfonic groups, although the same sulfonating chemicals were used. During direct sulfonation, thiol groups are directly linked to the silica framework, while in the post functionalization case, the thiol groups are replacing silanol groups on the silica surface [38]. While it is unlikely that thiol or sulfonic groups below the surface being directly exposed during titration or initial reaction times, the dissolution of the

porous surface will expose new sulfonic groups in direct sulfonated materials (SBA-15-DS) while the functional group will be leached upon dissolution in the post functionalizated material (SBA-15-PS). After an 8 h cycle, only ~15 % of the silica catalyst can be recovered, which indicates that the majority of the catalyst has been dissolved, and the sulfonic acid groups in the walls of SBA-15-DS have been exposed and increases the efficiency of the catalyst. The catalytic activity of SBA-15 without sulfonic groups is low, and corresponds to the reaction without a catalyst present.

Figure 5 (b) shows the conversion of catalysts containing carbon. The SBA-15 based materials show a better performance compared to the unordered porous carbon. Their fast initial rates are striking (see Table 2) and they all have a maximum conversions above 75 %. This occurs despite the differences in the concentration of catalytic groups (see Table 1), which suggest that equilibrium conditions for the reaction have been reached. Water is a side product of the esterification, and it may bind to silanol groups. Such situation favours a reverse hydrolysis reaction and lower the ester yield [4]. SBA-15-Carb2 has less silanol groups on the catalyst surface resulting in a slightly higher performance.

To elucidate the difference in performance of PC and SBA-15-Carb2, the turnover number, TON, was calculated by rationing the conversion with the amount of catalytic sulfonic groups (Figure 5 (d)-(f)), as well as the initial conversion rate (Table 2). It is apparent that the initial rates for PC and SBA-15-Carb2 differ significantly. The difference between these materials is the pore structure and the good diffusion through the cylindrical pores of SBA-15-Carb2 results in a better catalytic performance than PC, where the diffusion takes place through a complex network of narrow pores and micropores. This behaviour is consistent with previous studies showing better catalytic performance for mesoporous silica with larger pores compared to identical structures with smaller pores [11], as well as that interconnecting pores are favourable for the reaction [22].

It is clear that the conversion rate is faster and the maximum conversion higher for the carbon infiltrated SBA-15 materials compared to non-carbon infiltrated ones, see Table 2. The reasons for this are the higher amount of sulfonic groups in the carbon materials, and a stronger interaction between the sulfonic group and the reactants in the carbon based infiltrated materials. In the silicas, the sulfonic acid can interact with silanol groups, exposed during the dissolution of the material, and hence render a weaker acid compared to when the silanol groups are covered by the carbon layer as in SBA-15-Carb1 and SBA-15-Carb2 [39]. There can also be a confinement effect in the catalysts. The mesopores in the silica based and SBA-15-Carb materials are similar, and hence a the diffusion should be the same, but it is possible that the reagents reacting with the sulfonic acid groups in the interconnecting micropores in SBA-15-PS and SBA-15-DS gets trapped due to slow diffusion and hence decrease both the initial rate and maximum conversion. A slight positive confinement effect can also be observed in the carbon

based catalysts. Comparing SBA-15-Carb2 and SBA-15-RFC with similar initial rates, SBA-15-Carb2 has a lower acidic site density (Table 1). This indicates that the catalyst with cylindrical mesopores enables a higher conversion than free particles in the solution.

All the carbon containing materials and SBA-15-DS show better performance than the commercial solid acid catalysts (Figure 5 (d)).

3.3 Catalytic activity during transesterification of triglycerides (sunflower oil).

Since biodiesel production requires the transesterification of triglycerides with monohydric alcohols (methanol or ethanol), we tested the performance of the catalysts for the transesterification of a typical vegetable oil, sunflower oil for 8 h. The results presented in Figure 6 show that negligible conversions are achieved with commercial catalysts and silica materials without carbon. Only SBA-15-DS converts 0.02 % of the oil, and the others none. On the other hand, better conversions are achieved with SBA-15 based materials containing carbon. Remarkably, SBA-15-RFC shows a remarkably high conversion value of 85 %, while the non-ordered carbon (PC) has a conversion of 36 %.

It is apparent that the matrix holding the functional group strongly impacts the conversion of the sunflower oil. Comparing the conversions from the reactions catalysed by SBA-15-DS with SBA-15-Carb-2, which have similar pore characteristics and acidic group content gives a clear indication that the wetting of the matrix affect the catalysis. SBA-15-Carb2 contains a hydrophobic carbon surface inside the pores which should improve the wetting of the entire surface of the hydrophobic vegetable (sunflower) oil. To ascertain such effect, the different catalyst powders were dispersed in sunflower oil and the rate of sedimentation was measured. The catalysts containing carbon remain dispersed while the one of SBA-15 (silica) precipitates at a fast rate. (see, Fig S1 Supplementary Information). The SBA-15-RFC precipitates at an intermediate rate indicating that the presence of carbon improves the interaction with the hydrophobic reactant compared with to free silica (SBA-15). SBA-15-DS, and the other pore silica catalysts, are more hydrophilic. It results in poor wetting of the reactants and these catalysts are inactive.

The importance of wetting is also apparent for the carbon containing catalysts. SBA-15-Carb1 has a significantly higher amount of sulfonic acid groups compared the SBA-15-Carb2, with 0.87 mmol/g compared to 0.59 mmol/g respectively. If the materials were identical, SBA-15-Carb1 should give a higher conversion due to the higher concentration of catalytic sites. However, SBA-15-Carb1 contains less carbon in the pores and it is reasonable to assume that this material has some parts of the pore walls not covered by carbon. These uncovered parts will not be wetted by the sunflower oil and make

the catalyst less effective. The higher carbon coverage of the walls in SBA-15-Carb2 enables a more complete wetting. The lower degree of wetting in SBA-15-Carb1 results in a lower conversion despite having a higher concentration of functional groups compared to SBA-15-Carb2.

PC and SBA-15-Carb2 have similar amounts of sulfonic acid groups resulting in similar conversion, 36 and 30 % respectively. The small difference can also here be related to the silica support of the SBA-15 based catalyst. Similar trends have been observed by Alonso *et al*. [15], who observed that the rate of transesterification decreases when increasing the length of the alkyl chains. This was explained by steric hindrances, and repulsion between the non-polar ester chains, the polar acid groups on the catalyst's surface, and methanol in the pores.

SBA-15-RFC displays an outstanding 85 % conversion. This catalyst is a mixture of mesoporous silica and carbon nanoparticles. Here the hydrophobic functionalized carbon nanoparticles contain all the active catalytic sites while the hydroxyl groups of the hydrophilic silica adsorb the water bi-product. The latter reduces the reverse hydrolysis reaction [17] and combined with the high concentration of sulfonic acid groups on the active carbon nanoparticles a very effective catalyst is achieved with a high FAEE yield.

From the presented study it is clear that the choice of matrix for the catalytic group is crucial for the catalyst functionality. The matrix interaction with the reactants and products strongly affects the performance of the catalyst. Both geometrical and chemical interactions must be considered.

4. Conclusions

The presented study shows that the choice of matrix for a catalyst is vital for the catalyst performance. Monodispersed SBA-15 particles were synthesized and successfully functionalized with sulfonic groups, either during or after the particle synthesis. Carbon based catalysts were produced by successful infiltration of furfuryl alcohol, forming a CMK-5 type structure, while RFC infiltration rendered a mixture between mesoporous silica and carbon nanoparticles. The method allows the synthesis of novel materials useful as heterogeneous catalyst for Fischer's esterification and transesterification. In both Fischer esterification of acetic acid and ethanol, and biodiesel production from triglycerides (sunflower oil) and ethanol, the matrix affects the reaction in several ways. All our synthesized catalysts outperform the commercially available Amberlite IR-120 and Nafion 117.

In the reaction with acetic acid, both the silica surface and the carbons are wetted by the reactants, but the carbon containing materials are more efficient due to a higher concentration of sulfonic groups on the surface. It was also shown that a good diffusion is needed for efficient reactions. This is achieved

in ordered mesopores and around carbon nanoparticles, while narrow, slit shaped pores are unfavourable for rapid diffusion. We also observed that direct oxidation of sulfonic groups render a more stable catalyst compared to post grafting, even though the number of acidic sites are comparable.

The ordered silica modified with sulfonated carbon (SBA-15-RFC) shows very good performance in sunflower oil esterification with a conversion of 85 %. This is due to the combination of good wetting of the carbon particles, good diffusion, and adsorption of the water biproduct on the silica surfaces reducing the reverse hydrolysis reaction. The presented study shows undoubtedly that the catalyst matrix can be a make it or break it point for the catalysts performance.

The synergic effect of silica ordered mesoporosity and carbon properties (hydrophobicity, availability of reactive sites) seems to be advantageous for the fabrication of effective catalysts. The effect could be useful for other reactions and/or for the fabrication of materials bearing other catalytic functional groups.

Acknowledgements

This work was supported by the SUMA2 Network Project, 7th Framework Program of the European Commission (IRSES Project Nr. 318903), enabling movability. E. Björk and M. Odén were financially supported by the Knut and Alice Wallenberg Foundation under contract KAW 2012.0083. C.A. Barbero D.F. Acevedo, G. Planes and M.S. Moreno are permanent research fellows of CONICET. L. Tamborini and P. Militello thank CONICET for graduate fellowships. The funding of FONCYT, CONICET, MinCyT-Cordoba and SECYT-UNRC is gratefully acknowledged.

References

[1] A. Corma, S. Iborra, A. Velty, Chemical Routes for the Transformation of Biomass into Chemicals, Chemical Reviews, 107 (2007) 2411-2502.
[2] D.Y.C. Leung, Y. Guo, Transesterification of neat and used frying oil: Optimization for biodiesel production, Fuel Processing Technology, 87 (2006) 883-890.
[3] G. Mohammadi Ziarani, N. Lashgari, A. Badiei, Sulfonic acid-functionalized mesoporous silica (SBA-Pr-SO3H) as solid acid catalyst in organic reactions, Journal of Molecular Catalysis A: Chemical, 397 (2015) 166-191.
[4] A.F. Lee, K. Wilson, Recent developments in heterogeneous catalysis for the sustainable production of biodiesel, Catalysis Today, 242, Part A (2015) 3-18.
[5] Z. Helwani, M.R. Othman, N. Aziz, J. Kim, W.J.N. Fernando, Solid heterogeneous catalysts for transesterification of triglycerides with methanol: A review, Applied Catalysis A: General, 363 (2009) 1-10.
[6] L.H. Tamborini, M.E. Casco, M.P. Militello, J. Silvestre-Albero, C.A. Barbero, D.F. Acevedo, Sulfonated porous carbon catalysts for biodiesel production: Clear effect of the carbon particle size on the catalyst synthesis and properties, Fuel Processing Technology, 149 (2016) 209-217.
[7] S.K. Kundu, A. Bhaumik, Pyrene-Based Porous Organic Polymers as Efficient Catalytic Support for the Synthesis of Biodiesels at Room Temperature, ACS Sustainable Chemistry & Engineering, 3 (2015) 1715-1723.
[8] S. Bhunia, B. Banerjee, A. Bhaumik, A new hypercrosslinked supermicroporous polymer, with scope for sulfonation, and its catalytic potential for the efficient synthesis of biodiesel at room temperature, Chemical Communications, 51 (2015) 5020-5023.
[9] D. Zhao, J. Feng, Q. Huo, N. Melosh, G.H. Fredrickson, B.F. Chmelka, G.D. Stucky, Triblock copolymer syntheses of mesoporous silica with periodic 50 to 300 angstrom pores, Science, 279 (1998) 548-552.
[10] P. Gholamzadeh, G. Mohammadi Ziarani, N. Lashgari, A. Badiei, P. Asadiatouei, Silica functionalized propyl sulfonic acid (SiO2-Pr-SO3H): An efficient catalyst in organic reactions, Journal of Molecular Catalysis A: Chemical, 391 (2014) 208-222.
[11] J.P. Dacquin, A.F. Lee, C. Pirez, K. Wilson, Pore-expanded SBA-15 sulfonic acid silicas for biodiesel synthesis, Chemical Communications, 48 (2012) 212-214.
[12] M.L. Testa, V. La Parola, A.M. Venezia, Transesterification of short chain esters using sulfonic acid-functionalized hybrid silicas: Effect of silica morphology, Catalysis Today, 223 (2014) 115-121.
[13] S. Jeenpadiphat, E.M. Björk, M. Odén, D.N. Tungasmita, Propylsulfonic acid functionalized mesoporous silica catalysts for esterification of fatty acids, Journal of Molecular Catalysis A: Chemical, 410 (2015) 253-259.
[14] E.M. Björk, F. Söderlind, M. Odén, Single-pot synthesis of ordered mesoporous silica films with unique controllable morphology, Journal of colloid and interface science, 413 (2014) 1-7.
[15] D.M. Alonso, M.L. Granados, R. Mariscal, A. Douhal, Polarity of the acid chain of esters and transesterification activity of acid catalysts, Journal of Catalysis, 262 (2009) 18-26.
[16] M. Kruk, M. Jaroniec, T.-W. Kim, R. Ryoo, Synthesis and Characterization of Hexagonally Ordered Carbon Nanopipes, Chemistry of Materials, 15 (2003) 2815-2823.
[17] X. Wang, R. Liu, M.M. Waje, Z. Chen, Y. Yan, K.N. Bozhilov, P. Feng, Sulfonated Ordered Mesoporous Carbon as a Stable and Highly Active Protonic Acid Catalyst, Chemistry of Materials, 19 (2007) 2395-2397.
[18] L.H. Tamborini, M.P. Militello, J. Balach, J.M. Moyano, C.A. Barbero, D.F. Acevedo, Application of sulfonated nanoporous carbons as acid catalysts for Fischer esterification reactions, Arabian Journal of Chemistry, (2015).
[19] E.M. Johansson, M.A. Ballem, J.M. Córdoba, M. Odén, Rapid Synthesis of SBA-15 Rods with Variable Lengths, Widths, and Tunable Large Pores, Langmuir, 27 (2011) 4994-4999.
[20] E.M. Björk, F. Söderlind, M. Odén, Tuning the Shape of Mesoporous Silica Particles by Alterations in Parameter Space: From Rods to Platelets, Langmuir, 29 (2013) 13551-13561.

[21] E.M. Johansson, J.M. Córdoba, M. Odén, The effects on pore size and particle morphology of heptane additions to the synthesis of mesoporous silica SBA-15, Microporous and Mesoporous Materials, 133 (2010) 66-74.
[22] C. Pirez, J.-M. Caderon, J.-P. Dacquin, A.F. Lee, K. Wilson, Tunable KIT-6 Mesoporous Sulfonic Acid Catalysts for Fatty Acid Esterification, ACS Catalysis, 2 (2012) 1607-1614.
[23] D. Margolese, J.A. Melero, S.C. Christiansen, B.F. Chmelka, G.D. Stucky, Direct Syntheses of Ordered SBA-15 Mesoporous Silica Containing Sulfonic Acid Groups, Chemistry of Materials, 12 (2000) 2448-2459.
[24] M.M. Bruno, N.G. Cotella, M.C. Miras, C.A. Barbero, A novel way to maintain resorcinol–formaldehyde porosity during drying: Stabilization of the sol–gel nanostructure using a cationic polyelectrolyte, Colloids and Surfaces A: Physicochemical and Engineering Aspects, 362 (2010) 28-32.
[25] X. Mo, D.E. López, K. Suwannakarn, Y. Liu, E. Lotero, J.G. Goodwin Jr, C. Lu, Activation and deactivation characteristics of sulfonated carbon catalysts, Journal of Catalysis, 254 (2008) 332-338.
[26] A. Aldana-Pérez, L. Lartundo-Rojas, R. Gómez, M.E. Niño-Gómez, Sulfonic groups anchored on mesoporous carbon Starbons-300 and its use for the esterification of oleic acid, Fuel, 100 (2012) 128-138.
[27] M. Kruk, M. Jaroniec, A. Sayari, Application of large pore MCM-41 molecular sieves to improve pore size analysis using nitrogen adsorption measurements, Langmuir, 13 (1997) 6267-6273.
[28] E.P. Barrett, L.G. Joyner, P.P. Halenda, The Determination of Pore Volume and Area Distributions in Porous Substances. I. Computations from Nitrogen Isotherms, Journal of the American Chemical Society, 73 (1951) 373-380.
[29] J.K. Satyarthi, D. Srinivas, P. Ratnasamy, Influence of Surface Hydrophobicity on the Esterification of Fatty Acids over Solid Catalysts, Energy & Fuels, 24 (2010) 2154-2161.
[30] D. Srinivas, J.K. Satyarthi, Biodiesel Production from Vegetable Oils and Animal Fat over Solid Acid Double-Metal Cyanide Catalysts, Catalysis Surveys from Asia, 15 (2011) 145-160.
[31] S. Soll, M. Antonietti, J. Yuan, Double Stimuli-Responsive Copolymer Stabilizers for Multiwalled Carbon Nanotubes, ACS Macro Letters, 1 (2012) 84-87.
[32] M. Cournil, F. Gruy, P. Gardin, H. Saint-Raymond, Modelling of solid particle aggregation dynamics in non-wetting liquid medium, Chemical Engineering and Processing: Process Intensification, 45 (2006) 586-597.
[33] H.P. Boehm, Surface oxides on carbon and their analysis: a critical assessment, Carbon, 40 (2002) 145-149.
[34] H. Im, B. Kim, J.W. Lee, Concurrent production of biodiesel and chemicals through wet in situ transesterification of microalgae, Bioresource Technology, 193 (2015) 386-392.
[35] X.Y. Bao, X.S. Zhao, Morphologies of Large-Pore Periodic Mesoporous Organosilicas, Journal of Physical Chemistry B, 109 (2005) 10727-10736.
[36] L.M. Yang, Y.J. Wang, G.S. Luo, Y.Y. Dai, Simultaneous removal of copolymer template from SBA-15 in the crystallization process, Microporous and Mesoporous Materials, 81 (2005) 107-114.
[37] L.M. Yang, Y.J. Wang, G.S. Luo, Y.Y. Dai, Functionalization of SBA-15 mesoporous silica with thiol or sulfonic acid groups under the crystallization conditions, Microporous and Mesoporous Materials, 84 (2005) 275-282.
[38] M.L. Testa, V. La Parola, A.M. Venezia, Esterification of acetic acid with butanol over sulfonic acid-functionalized hybrid silicas, Catalysis Today, 158 (2010) 109-113.
[39] J.-P. Dacquin, H.E. Cross, D.R. Brown, T. Duren, J.J. Williams, A.F. Lee, K. Wilson, Interdependent lateral interactions, hydrophobicity and acid strength and their influence on the catalytic activity of nanoporous sulfonic acid silicas, Green Chemistry, 12 (2010) 1383-1391.

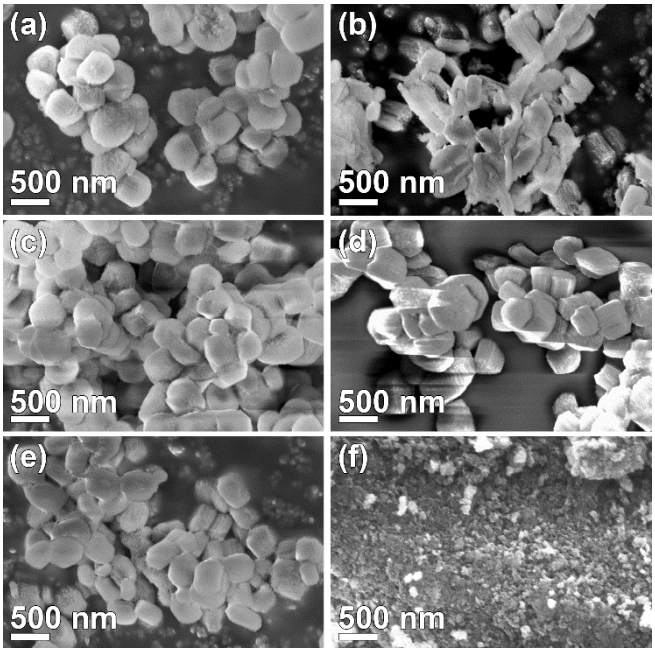

Figure 1. SEM micrographs of (a) pure

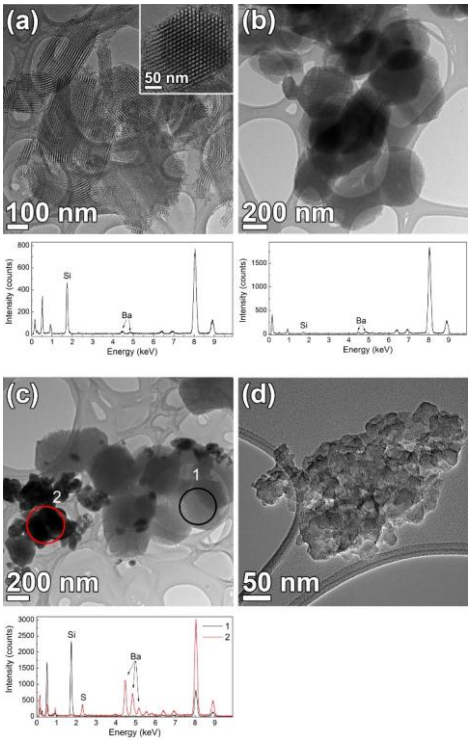

Figure 2. TEM micrographs and EDS spectra of the synthesized catalysts (a) SBA-15-DS, (b) SBA-15-Carb2, (c) SBA-15-RFC, and (d) PC.

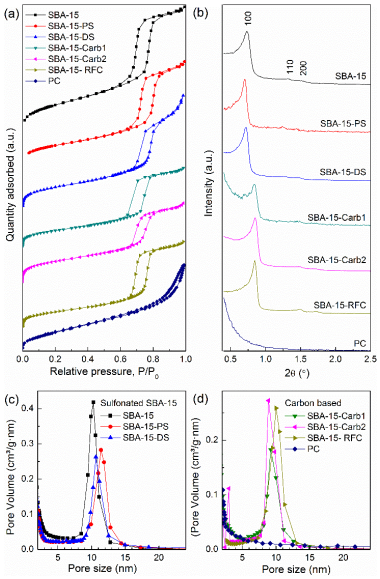

Figure 3. Physisorption isotherms (a) x-ray diffractograms (b), and pore size distributions (c) and (d) for the different catalysts. The isotherms are plotted as offset with respect to the y-axis.

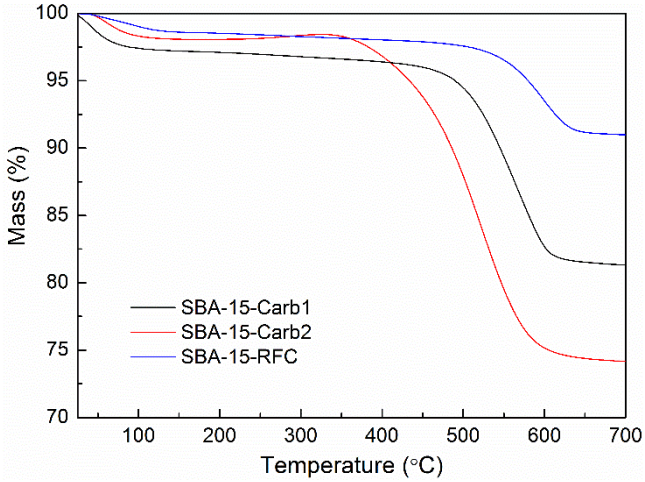

Figure 4. Thermogravimetric analysis of the carbon infiltrated SBA-15s.

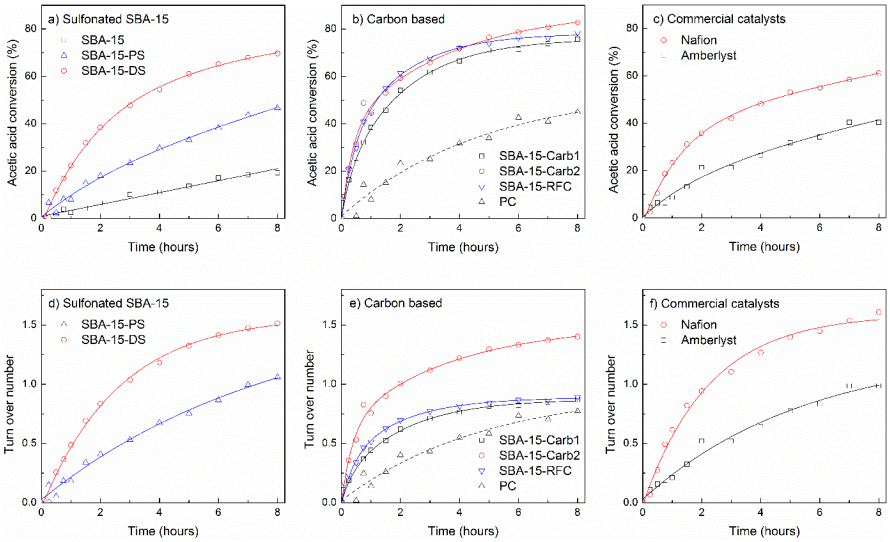

Figure 5. Catalytic efficiency (a) – (c) and turnover numbers (d) – (f) for the different catalysts in the esterification reaction of acetic acid and ethanol at 80 °C. SBA-15 materials without carbon (left), carbon based materials (center), and commercial solid acid catalysts (right).

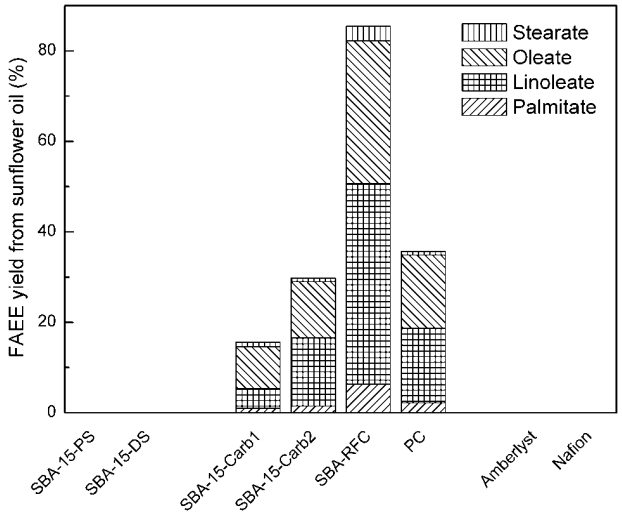

Figure 6. Results of transesterification of sunflower oil and ethanol using porous or commercial catalysts.

Table 1. Characteristics of the catalysts: physiochemical properties, amount of carbon, and number of acidic sites.

Material	Specific surface area [a] (m^2/g)	Pore size [b] (nm)	Total pore volume [c] (cm^3/g)	Unit cell parameter (nm)	Amount of carbon (wt%)	Acidic sites [d] (mmol/g)
SBA-15	583	10.5	0.95	13.6	-	0.26
SBA-15-PS	441	10.5	0.83	14.2	-	0.44
SBA-15-DS	417	10.7	0.88	14.0	-	0.46
SBA-15-Carb1	510	9.2	0.67	12.0	15.8	0.87
SBA-15-Carb2	355	8.9	0.63	11.9	24.3	0.59
SBA-15-RFC	340	10.0	0.71	11.9	7.6	0.86
PC	679	-	0.81	-	100	0.58
Nafion® 117	-	-	-	-	-	0.38[e]
Amberlite IR-120	-	-	-	-	-	0.41[e]

[a]Calculated with the BET method at $P/P_0 = 0.1 – 0.2$.
[b]Calculated using the KJS method for SBA materials and the BJH method for the porous carbon.
[c] Estimated at $P/P_0 = 0.98$.
[d]Determined using acid base titration.
[e]Data from suppliers

Table 2. Initial rates and the maximum conversion after 8 h for the catalysed Fischer esterification of ethanoic acid with acetic acid.

Material	Initial rate (%/h)	Maximum conversion (%)
SBA-15	2.93	21.1
SBA-15-PS	8.57	46.8
SBA-15-DS	19.3	69.5
SBA-15-Carb1	37.1	77.5
SBA-15-Carb2	46.7	83.0
SBA-15-RFC	44.4	74.8
PC	11.8	45.0
Nafion® 117	25.2	61.2
Amberlite IR-120	7.7	41.4